IEEE Access
Multidisciplinary | Rapid Review | Open Access Journal

Received August 1, 2019, accepted August 20, 2019, date of publication August 26, 2019, date of current version September 10, 2019.

Digital Object Identifier 10.1109/ACCESS.2019.2937600

A Novel Chaotic Flower Pollination Algorithm for Global Maximum Power Point Tracking for Photovoltaic System Under Partial Shading Conditions

DALIA YOUSRI[1], THANIKANTI SUDHAKAR BABU[2], (Member, IEEE), DALIA ALLAM[1], VIGNA K. RAMACHANDARAMURTHY[2], (Senior Member, IEEE), AND MAGDY B ETIBA[1]

[1]Electrical Engineering Department, Faculty of Engineering, Fayoum University, Fayoum 63514, Egypt
[2]Department of Electrical Power Engineering, Institute of Power Engineering, Universiti Tenaga Nasional, Kajang 43000, Malaysia

Corresponding author: Thanikanti Sudhakar Babu (sudhakarbabu66@gmail.com)

This work was supported by the Universiti Tenaga Nasional (UNITEN), Malaysia, through INTERNAL RESEARCH GRANT OPEX under Grant RJO10436494.

ABSTRACT A partial shading condition is an environmental phenomenon that causes multiple peaks in Photovoltaic (PV) characteristics. Introducing robust and reliable Maximum Power Point Tracking technique is essential in PV systems to extract the Global Maximum Power Point (GMPP) irrespective of the environmental conditions. Therefore in this manuscript, a novel optimization algorithm is implemented for MPPT. The developed technique named Chaotic Flower Pollination Algorithm (C-FPA) merges the chaos maps (Logistic, sine, and tent maps) to tune the basic algorithm parameters adaptively. The effectiveness of the introduced variants is proved using several patterns of partial shading condition. Moreover, these variants are certified for tracking the GMPP in case of dynamic and sudden variation in the irradiance conditions. Several statistical analysis is carried out to evaluate the performance of the proposed variants in comparison with the standard version of the Flower Pollination Algorithm (FPA). The significant outcome clarifies that combining the chaos maps with FPA improves the dependability and stability of the FPA and offers higher tracking efficiency with a reduction of tracking time by 50% when compared to FPA. Moreover, the proposed C-FPA provides a better dynamic response, especially with the tent chaos map.

INDEX TERMS Chaos maps, flower pollination algorithm, maximum power point tracker, partial shading conditions.

I. INTRODUCTION

Increase in energy demand and the depletion of non-renewable energy resources brings a new challenge to the power industry sector. Solar energy is highly popular due to its wide range of features like minimal maintenance, noise-free, environmentally friendly, and abundant in nature [1]. Additionally, the installation costs of PV plants are reducing due to the rapid growth in PV technology [2]. However, solar PV has limitations and challenges due to its non-linear nature, low output power efficiency, life span, and power generation that mostly depends on climatic conditions like irradiation and temperature. The effect of partial shading and power generation of a PV system under various shade conditions are clearly explained in Section II-A. To enhance its efficiency, various researchers introduced maximum power point extraction techniques, to extract the maximum power by operating a non-linear system at a unique operating point widely known as a maximum power point (MPP). With this inspiration to provide a solution for partial shading condition, the massive number of maximum power point extraction techniques have evolved. MPPT can be broadly categorized into two types, namely hardware based reconfiguration MPPT techniques, and firmware based MPPT techniques.

The hardware-based reconfiguration techniques comprise of PV array reconfiguration [3], [4], differential power processing (DPP) [5] and DC optimizer methods [6]. Although these methods show excellent performance, there are

The associate editor coordinating the review of this article and approving it for publication was N. Prabaharan.

limitations such as it requires additional switching devices, skilled persons, and long cables to avoid crossing between PV modules [3]. DPP and DC optimizer methods require a high number of DC-DC converters to control the generated power and difference of power between various PV modules [7]. On the other hand, firmware-based MPPT techniques were widely developed and implemented to achieve GMPP without any additional switching units and sensors. Thereby, it reduces system cost and easy to implement. These methods are classified into three major types, namely traditional, evolutionary based algorithms, and artificial intelligence methods.

The traditional MPPT techniques [8] suffer from weak convergence, settles at LMPP during shade conditions and generates oscillations around MPP. Also, these methods are only suitable for uniform irradiation conditions [9]. To tackle these drawbacks and to track MPP even under any irradiation, numerous authors developed soft computing techniques using artificial intelligence or bio-inspired techniques.

The bio-inspired algorithms have been widely used due to their extensive features like, solving non-linear multi-model optimization problems effectively, with faster convergence rate, quick response with a wide range of exploration in the search which guarantees to track the GMPP under any environmental conditions [10]. The well-known algorithms developed in recent years for the application of MPPT are Bat algorithm [11], moth-flame optimization (MFO) algorithm [12], flower pollination algorithm (FPA) [13], nonlinear backstepping method [14], golden search-based method [15], Fireworks algorithm [16], wind-driven optimization (WDO) algorithm [17], mine blast optimization (MBO) and teaching learning-based optimization (TLBO) algorithms [18]. The other meta-heuristic algorithms are grey wolf optimization (GWO), moth-flame optimization (MFO), salp swarm algorithm (SSA) and hybrid particle swarm optimization-gravitational search Algorithm (PSO-GSA) which are implemented in [19] to handle partial shading conditions towards achieving GMPP.

As MPPT becomes an attractive topic, the improved versions of bio-inspired algorithms were proposed similar to improved versions of traditional methods. That are namely, modified particle swarm optimization [1], improved differential evolution algorithm [20] and modified cat swarm optimization (MCSO) [21]. Further, the authors introduced hybrid algorithms by combining the features of one or more algorithms, namely variable perturbation frequency (VPF) [22] with P&O and PSO. In [23], by combining the features of PSO variants with HC algorithm, authors proposed simplified accelerated particle swarm optimization (SAPSO). Accelerated particle swarm optimization is proposed in [24] by considering P&O and basic PSO to overcome longer convergence time. Hybrid Gaussian process regression-jaya (GPR-Jaya) algorithm was introduced in [9], whereas a comprehensive improvement on the artificial fish swarm algorithm (CIAFSA) was proposed in [25]. Hybrid grey wolf optimization with fuzzy logic control (GWO-FLC) method was reported in [26]. TSPSOEM is proposed by combing the algorithms PSO and shuffled frog leaping algorithm (SFLA) in [27]. From the extensive research done by various researchers, the noticeable remarks and limitations of their methods are presented in Table 1. The commonly observed limitations of the above algorithms are less consistency to achieve MPP, fails to reach GMPP under a rapid and dynamic change in irradiation, adaptive step method consumes more time to meet GMPP, and performance slow in convergence [34]. Some of the bio-inspired algorithms exhibit very less trade-off between exploitation and exploration, which cause fluctuations around MPP and settles at LMPP during high shade conditions [17]. Due to the drawbacks as mentioned earlier, PV system tracks very less amount of power; which greatly effects, the efficiency and payback period. Additionally, from the comparative Table 1, it is observed that most of the researchers improved the performance of algorithms by tuning some parameters and many of them failed to consider their method under dynamic irradiation conditions. Besides, very few authors considered the statistical analysis to exhibit the efficiency of their techniques. The other significant gap noticed from the literature is, none of the researchers attempted to introduce chaotic behavior in the application MPPT which will dramatically enhance the performance of the optimization algorithms when dealing with non-linear objectives [35]–[38].

Therefore in this article, authors proposed the chaos theory into optimization algorithms. By recognizing the dynamic and randomization features of chaos maps, optimization algorithms maintain a perfect trade-off between exploration and exploitation process [35], [36]. With this motivation, authors in this article introduced variants of chaotic optimization algorithm for the application MPP irrespective of the environmental conditions, including with various dynamic shade patterns. By introducing the chaotic behavior to the conventional FPA, the proposed algorithm is named as novel chaotic flower pollination algorithm (C-FPA). In this method, three well known chaotic maps; logistic, sine, tent maps are considered along with basic FPA. The main features of this article can be summarized as follows;

- A novel method of chaotic FPA variants with logistic, sine tent chaos maps are introduced to achieve global maximum power point.
- The performance of the proposed method is evaluated under uniform and dynamic change in irradiation conditions over a PV string 4S configuration designed with Shell S36 module.
- The obtained results exhibit the superiority of chaos maps in-terms of convergence speed, tracking MPP without any steady state oscillations, high consistency and efficiency compared to basic FPA.
- Applicability of the proposed chaos variants are supported by statistical analysis and recommends the best chaos map that tracks GMPP under uniform and dynamic change in irradiation conditions.

TABLE 1. Comprehensive study on recently published algorithms for MPPT.

Ref	Year	Algorithm	Testing Conditions			Statistical Analysis	Comments/Observations
			Uniform shading	Partial shading	Dynamic shading		
[22]	2019	Hybrid PSO and P&O	✓	✓	✓	✗	Achieved maximum efficiency of 96.7%. Considered configuration was 5S. The initial duty cycles were chosen directly without proper procedure.
[28]	2019	Hybrid ELPSO-P&O	✗	✓	✓	✗	Implemented for 3S2P, 4S2P configurations. Author did not calculate efficiency of the system.
[29]	2019	Tangents perturbation on P-V characteristics	✓	✓	✓	✗	The method was tested over 2S, 2S2P and 3S3P configurations. Attained max efficiency of 97.8% and consumes 19 cycles to achieve MPP. Authors compared their method over traditional P&O.
[24]	2019	Accelerated PSO i.e., (Hybrid PSO and P&O)	✗	✓	✓	✗	This method taking 2.4 sec during uniform irradiation condition to reach GMPP and reached maximum efficiency of 99%. Tested for only one configuration.
[30]	2019	IPSO and P&O	✗	✓	✓	✗	The system tested under 2S configuration of power rating 70 W each panel. The proposed method was compared with PSO and P&O. Authors did not verified robustness and consistency of algorithm
[31]	2019	Adaptive perturbation frequency	✓	✗	✗	✗	The method was tested with single PV module of 14.6 W. Authors not considered partial shade conditions and the results are not compared with any other method.
[19]	2019	GWO, MFO,SSA and Hybrid PSO-GSA	✓	✓	✗	✓	A 4S3P configuration was used to test the algorithms, robustness of methods were presented based on the metrics performed. Efficiency of PSO-GSA was higher than other algorithms
[9]	2019	Hybrid GPR-JAYA	✗	✓	✗	✗	In this, authors used controlled voltage source, in place of converter, thereby, this method is not much effective, towards controlling the duty cycles like regular method.
[32]	2019	P&O- ABC	✗	✓	✓	✗	This method was implemented for 2S configuration with maximum rated power capacity of 74W. Implementing hybrid algorithm for configuration of 2S was not much effective. Achieved efficiency of 99.59% in 0.08 sec in tracking and it was compared with P&O, INC and ABC
[33]	2019	PSO-RBFNN	✓	✗	✗	✗	This method was implemented with 2 series PV modules, with rated capacity of 37 W each. The attained efficiency was 99.04%.
[26]	2019	Hybrid GWO-FLC	✗	✓	✓	✗	Authors followed predefined time or occurrence of PSC to re-initializing the searching agents; pre-defining time was not so accurate. Achieved efficiency of 99.99% for hybrid algorithm using predefined time initialization concept.
[17]	2019	WDO	✓	✓	✗	✓	The developed algorithm was tested with 4S configuration, and statistical comparative study was carried-out using various existing algorithms like PSO, DE, HSA, Bat, SCA, CS and GA.
[27]	2018	TSPSOEM	✗	✓	✓	✗	This algorithm was proposed for DMPPT for a large number of interconnected converter configurations with combination of permutation algorithm. This system utilizes the variable converter ratios and reduces the shading effect and tested over a grid connected system.
[23]	2018	HSAPSO	✓	✓	✓	✗	In this method authors divided a single PV module into two individual PV modules and integrated 2x33 photovoltaic cells to each other. The configuration was made as 2S with single PV module. The proposed method was compared with basic version of PSO.
[13]	2017	FPA	✓	✓	✓	✗	Authors evaluated the performance of FPA over P&O and PSO. PV array of 4S configuration was developed and attained the efficiency of 99.85%. The authors performed a single run to evaluate the performance, but it not guarantees the robustness of the method.

The remaining sections of the article are organized as follows; Section II details the selection and modeling of PV cell with basic design equations. The effect of partial shade and its characteristics are discussed in section II-A. Section III introduces the proposed optimization algorithm variants, the employed chaos maps and implementation steps for the application of MPPT. Section IV presents the analysis and the result of the proposed variants and basic FPA towards achieving GMPP. Finally, section V summarizes the primary outcomes and the conclusions.

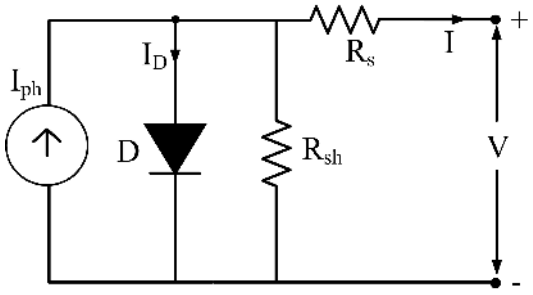

FIGURE 1. Equivalent circuit of single diode PV model.

II. PHOTOVOLTAIC MODELS

The modeling of PV cell is considered as high priority by numerous researchers, since, the nonlinear characteristics and change in environmental conditions greatly effects the performance of PV cell. The accurate PV cell can be developed with the help of single or double diode models. Single diode model (SDM) is popular due to its accuracy, easier to design and involves less parameters [1]. The electrical equivalent circuit of SDM is shown in Fig. 1. It consists of current source (I_{ph}), diode D, series resistance (R_s) and shunt resistance (R_{sh}). The (R_s) and (R_{sh}) exhibits contact and leakage losses respectively [1]. By applying KCL to the equivalent circuit, the total current produced by PV cell can be given as in (1).

$$I = I_{ph} - I_o\left[exp\left(\frac{(V + IR_s)}{aV_t}\right) - 1\right] - \frac{(V + IR_s)}{R_{sh}} \quad (1)$$

where I_{ph}, I_o, R_s, and R_{ph} are respectively PV current, leakage current, series and shunt resistance. a and V_t represent ideality factor of a diode D and thermal voltage respectively and it can be given as $V_t = \frac{N_s kT}{q}$. Here, k is Boltzmann constant and its value is $1.35 * 10^{-23} J/K$, T is temperature of a PV cell in Kelvin, q and N_s are charge of electron (1.6×10^{-19} C) and number of cells in series. I_{ph} and I_o can be calculated by

using (2) and (3)

$$I_{ph} = [I_{ph_{STC}} + k_i(T - T_{STC})]\frac{G}{G_{STC}} \tag{2}$$

where k_i is coefficient of short circuit current, $I_{ph_{STC}}$ represents pv current under standard test conditions (STC) i.e., $25°C$ and $1000W/m^2$.

$$I_o = \frac{I_{SC-STC} + k_i(T - T_{STC})}{exp\left(\frac{(Voc-STC)+k_v(T-T_{STC})}{nv_T}\right) - 1} \tag{3}$$

where k_v is coefficient of open circuit voltage, I_{SC-STC} and V_{OC-STC} are the short circuit current and open circuit voltage under STC respectively. To compute the total current produced by PV module under partial shading effect 1 can be rewritten as in 4.

$$I = N_{pp}\left\{I_{ph} - I_o\left[exp\left(\frac{(V + IR_s)}{aV_tN_{ss}}\right) - 1\right]\right\} - \frac{(V + IR_s)}{R_{sh}} \tag{4}$$

where N_{pp}, N_{ss} represents the number of parallel and series connected PV modules.

A. PARTIAL SHADING AND ITS EFFECTS

The PV plant is designed with PV modules connected in series and parallel to meet the required load [4]. Further, due to the presence of passing clouds, bird droppings, building shadows and dust, all PV panels may not receive an equal amount of irradiation [1]. Hence, it results in uneven irradiance known as partial shading. With this scenario, the current generated by the PV string is equal to the current generated by the shaded PV panel. Besides, the shaded PV panel loses its capability to generate current, and the temperatures of that particular panel increases, which causes hot-spots, thus damaging the PV panels. To overcome this drawback, a bypass diode can be connected across each panel. To understand the effect of partial shading in detail, in this article, authors considered three different shading patterns over a string of 4 PV panels connected in series (4S), designed with Shell S36 PV module. The specifications of the S36 PV module are presented in Table 2.

TABLE 2. Specifications solar S36 PV module.

Parameters	S36
Type of cell	Multi-crystalline
Rated power	36 W
Peak power voltage (V_{mpp})	16.5 V
Peak power current (I_{mpp})	2.18 A
Open circuit voltage (V_{oc})	21.4 V
Short circuit current (I_{sc})	2.30 A
Current temperature coefficient (k_i)	$0.001A/K$
Voltage temperature coefficient (k_v)	$-0.76V/K$
No. of series cells	36
Cell dimensions	125.0×62.5

For each string, a blocking diode is connected to avoid the reverse flow of current. The three different shade patterns are shown in Fig. 2(a) and are as follows;

1) Pattern 1: Zero shade condition. In this pattern, all the PV panels (M_1, M_2, M_3, M_4) will receive equal irradiation ($1000W/m^2$). All the PV panels will generate an equal amount of current. Therefore, it generates a P-V curve with a single peak with maximum power. The single peak is considered as GMPP, which is represented as $P1$ in P-V curves of Fig. 2(b).
2) Pattern 2: Partial shade condition. In this pattern, module M_1, M_2 receives 1000 W/m^2 and M_3, M_4 receives 300 W/m^2. Due to the occurrence of shade over PV modules M_3, M_4, the current generated by the PV string will be equal to shaded PV modules current.

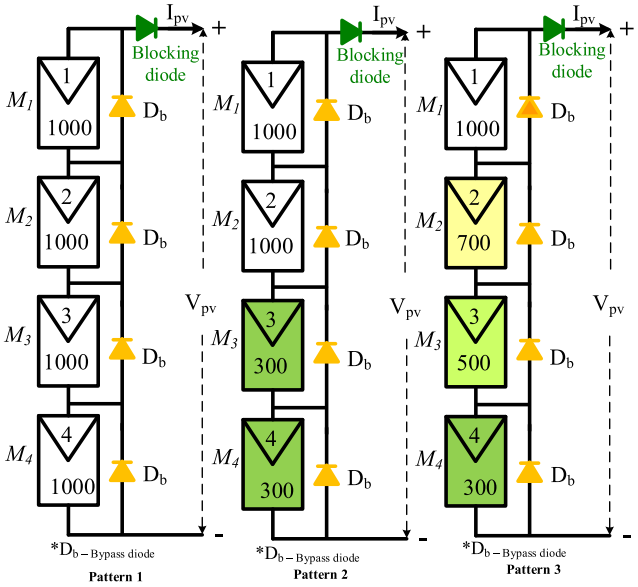

(a)

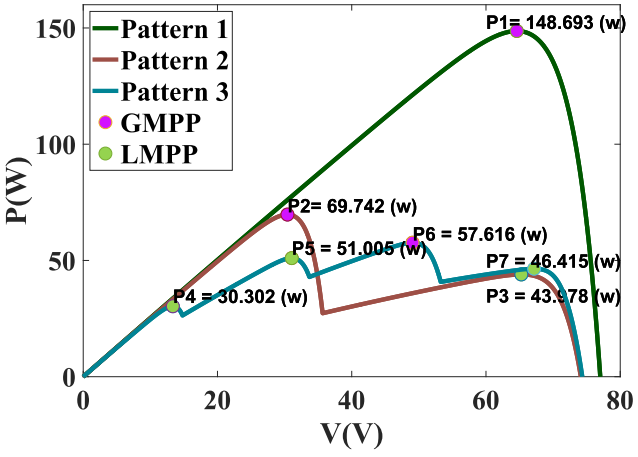

(b)

FIGURE 2. Partial shading analysis on S36 PV module (a) Shading patterns, and (b) P-V curves.

Moreover, the presence of a bypass diode across each panel will help to bypass the maximum current generated by un-shaded PV panels. Due to this difference in currents, it will generate two different peaks in P-V curves, which are represented with P_2 and P_3, as shown in Fig. 2(b). The point P_2 and P_3 are known as a local maximum power point (LMPP) and global maximum power point (GMPP) for pattern 2.

3) Pattern 3: Strong shade condition. In this pattern, the PV modules M_1, M_2, M_3 and M_4 receives 1000 W/m^2, 700 W/m^2, 500 W/m^2, 300 W/m^2 respectively. The four PV modules receive four different shades, whereby each panel develops its own current based on shades. Hence, it generates multiple peaks on P-V curves. Its points are represented as P_4, P_5, P_6 and P_7 in Fig. 2(b). In these four peaks, only one point (P_6) is known as GMPP, and other points are considered as LMPP.

Hence, due to partial shade conditions, there exist multiple peaks over P-V curves. The conventional and other evolutionary based algorithms will have difficulty to reach GMPP due to the presence of multiple peaks. The power generating capacity reduces greatly, thus affecting the performance of the PV plant. Hence, in this article, the authors presented a novel and robust MPPT technique with chaotic variants of FPA to track maximum power irrespective of any shade conditions.

III. IMPLEMENTING CHAOTIC FLOWER POLLINATION ALGORITHM AS MPPT

The Flower Pollination Algorithm (FPA) was widely utilized in several applications and has shown its superiority over particle swarm optimizer and genetic algorithm [39]–[41]. Yang developed FPA via emulating the mating process in the plants [42]. The biological evolution in the flowers is implemented in FPA technique, where the main purpose is the survival of the best and with the most optimum reproduction. Unfortunately, the control parameters of FPA and the initialization of the population's size have a large impact on its performance. Therefore, a new approach was discussed to replace these parameters with chaos maps to provide adaptive tuning of these parameters. As a result, the chaotic flower pollination algorithm is introduced. In the current work, three chaos maps included logistic, sine, and tent maps are merged with FPA to implement maximum power point tracking. The implementation details of C-FPA as MPPT is discussed in the following subsection.

A. CHAOTIC FLOWER POLLINATION ALGORITHM VARIANTS (C-FPA)

The pollination in plants inspires FPA. The biological aim from this process is the survival of the fittest species and the most optimum reproduction. To achieve this biological target, the pollination process occurs via biotic or abiotic processes. In the biotic process, the bats, honey bees and insects transfer the pollen between two different flowers while abiotic process concerns with the self-pollination process where the pollen is transferred from one flower to fertilize the same flower [42]. The mathematical representation for these processes is modeled as follows.

In FPA algorithm, it is assumed that the global pollination occurred during the biotic process and can be mathematically represented as follows:

$$U_i^{T+1} = U_i^T + \gamma L(\lambda)(G_* - U_i^T), \tag{5}$$

where U_i^T indicates the solution vector i at iteration T, the G_* is the global solution happened so far. γ is a scaling factor to control the step size. $L(\lambda)$ is the levy factor responsible for the transfer of pollen between different species of flowers and it is computed as follows [42]:

$$L(\lambda) \sim \frac{\lambda\Gamma(\lambda)\sin(\frac{\pi\lambda}{2})}{\pi}\frac{1}{d^{1+\lambda}} \qquad (d \gg d_o > 0), \tag{6}$$

where $\Gamma(\lambda)$ is the gamma function. This approximation is proved for large steps, $d > 0$ as d is step size and the value of d_o can be as small as 0.1 [42].

The abiotic process is recognized for the local pollination process and is formulated as follows [42]:

$$U_i^{T+1} = U_i^T + \epsilon(U_l^T - U_k^T), \tag{7}$$

where U_l^T, U_k^T are two different pollens of same plant species, and ϵ is drawn from a uniform distribution $\in [0, 1]$. In FPA, the transformation between the global an local pollination process is controlled by a switching probability factor, S_W, where its values was selected in the interval $\in [0.2, 0.8]$ [42].

Based on the descriptive equation for the FPA algorithm, it is obvious that the motion and the solution of the populations are controlled by parameters such as S_W and ϵ. Moreover, the initialization of the population influences the search space and behavior of FPA. In FPA, Gaussian and uniform distributions are utilized to generate these parameters and the initialization process. In literature, it was proved that employing the chaos systems with the meta-heuristic algorithms in the place of the uniform and Gaussian distributions enhance their consistency, accuracy, and convergence decaying rate [43]–[45]. The chaos has dynamic characteristics of ergodicity and randomness. Based on these features, the exploration phase of the algorithm is enhanced, and the convergence is prematurely avoided. Further, this method reduces the possible data redundancy [45]. Therefore, in the current work, the chaos maps are applied to identify the initial population, the probability switch (S_W) and ϵ of FPA. As a result, Chaotic Flower Pollination Algorithm (C-FPA) variants are introduced.

In this paper, three types of one dimensional chaos maps are employed. The utilized maps are Logistic, Sine and Tent chaos maps. Their mapping were expressed as follows:

- Logistic map [46]

$$x_{T+1} = bx_T(1 - x_T), \tag{8}$$

where x_T is the T^{th} chaotic number, T is the times of iteration, b is the control parameter of chaotic behavior and equals to 4, to ensure a complete chaotic state. x $\in$ (0,1) under the initial condition $x_0 \in (0,1)$. Therefore, x_0 is selected to be 0.7.

- Sine map [47] can be defined as follows:

$$x_{T+1} = \frac{a}{4} sin(\pi x_T) \tag{9}$$

where a is the control parameter of a chaotic behavior of sine map. Its value equals to 4. The initial condition, $x_0 = 0.7$.

- Tent map [36] can be expressed as follows:

$$x_{T+1} = \begin{cases} \dfrac{x_T}{0.7}, & x_T < 0.7 \\ \dfrac{10}{3}(1 - x_T), & x_T >= 0.7 \end{cases} \tag{10}$$

where the initial condition, $x_0 = 0.6$.

B. MPPT BASED ON CHAOTIC FLOWER POLLINATION ALGORITHM

Recognizing the advantages of merging the chaos maps with meta-heuristic optimization algorithms, authors in this paper have attempted to track GMPP for the first time. Thereby, it enhances the wide search range and prevents premature convergence. In the novel MPPT technique, the chaos maps are used to produce the initial population and to tune the parameters of a basic version of FPA. Therefore, it helps in increasing the performance in tracking GMPP during partial shade conditions. The flowchart of C-FPA optimizer of MPPT is shown in Fig. 3.

IV. SIMULATION AND RESULTS

To appraise the tracking performance of the novel C-FPA based MPP tracker, three different partial shading patterns are utilized. The dynamic and abrupt variation between the partial shade patterns is investigated as well to evaluate the robustness and stability of the proposed variants. Intensive comparison is carried between the C-FPA variants and the standard FPA to clarify the influence of utilizing the chaos maps for the first time in the MPPT system. The performance is compared in terms of tracking speed, tracking time, stability, and efficiency.

Further, an extensive statistical analysis is carried out over several intervals of simulation time to determine the consistency and reliability of the novel MPPT method. For a fair comparison, each algorithm is simulated for 10 independent runs. All the algorithm variants are coded and implemented on "MATLAB 2018" platform on a laptop with Core i7-6500U CPU, 2.5 GHz of speed and 4 GB of RAM.

The applied statistical analysis proves the effectiveness of the proposed algorithm. The performance factors considered are root mean square error (RMSE), mean absolute error (MAE) and standard Deviation (STD). The efficiency of used variants in tracking the maximum global power is

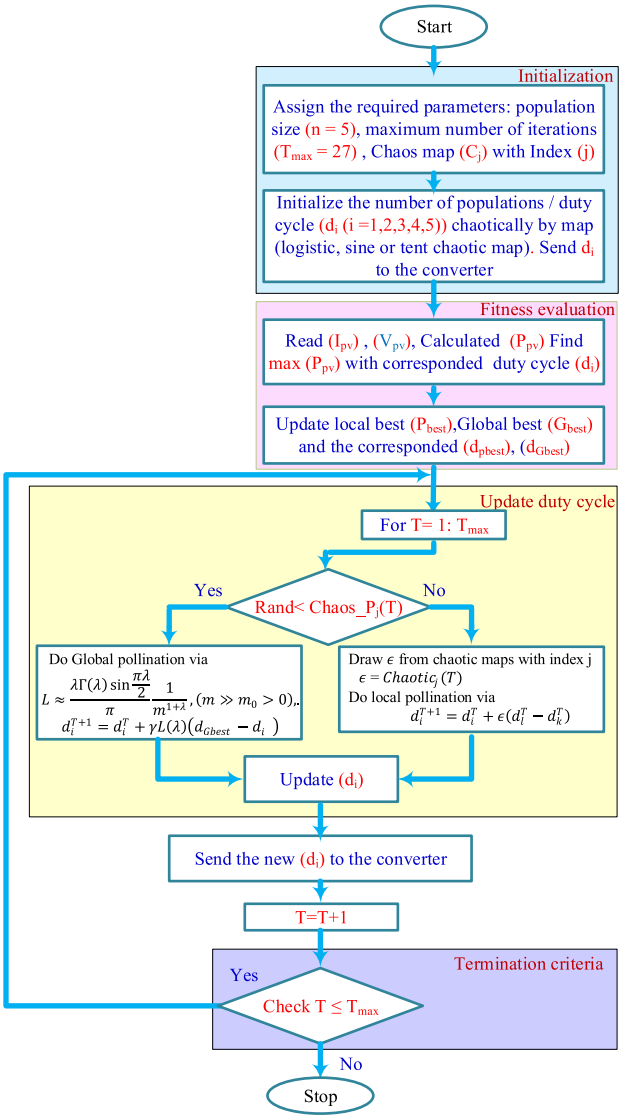

FIGURE 3. Flowchart of the C-FPA MPPT optimizer.

computed over several intervals of simulation time. The mathematical formula of these metrics are modeled as follow:-

Efficiency (η)

$$\eta = \frac{P_{pv_{ei}}}{P_{pv_m}} * 100\% \tag{11}$$

Root Mean Square Error (RMSE)

$$RMSE = \sqrt{\frac{\sum_{i=1}^{K} \left(P_{pv_{ei}} - P_{pv_m}\right)^2}{K}} \tag{12}$$

Mean Absolute Error (MAE)

$$MAE = \frac{\sum_{1}^{K} |P_{pv_{ei}} - P_{pv_m}|}{K} \tag{13}$$

Standard Deviation (STD)

$$STD = \sqrt{\frac{\sum_{i=1}^{K} \left(P_{pv_{ei}} - \hat{P_{pv_{ei}}}\right)^2}{K}}, \tag{14}$$

where $P_{pv_{ei}}$ and $\hat{P}_{pv_{ei}}$ are the average power over number of runs and it is calculated for each run (i). P_{pv_m} is the measured global PV power. K is the total number of the runs.

The schematic diagram of the developed MPPT system is shown in Fig. 4. It is composed of a DC-DC boost converter with input inductance is 30 mH, the output capacitor is 100 μF with load resistance 100 Ω. The sampling time between duty cycles is 0.03 sec.

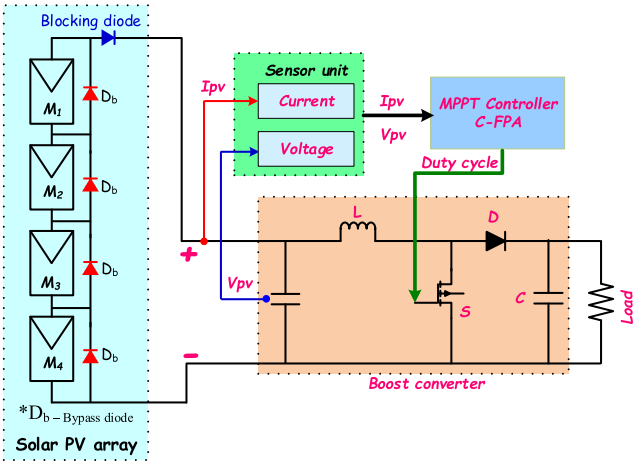

FIGURE 4. Schematic of the MPPT control system.

A. SIMULATION STUDY UNDER PARTIAL SHADING PATTERNS 1, 2 AND 3

In the first part of the discussions, the C-FPA is tested with the shade patterns as given in section. II-A and compared with FPA in terms of tracked power values, tracking speed, and efficiency in attaining GMPP. Statistical analysis is described in detail in the following subsections.

1) TRACKING SPEED AND ACCURACY STUDY

To study the reliability, efficiency, and accuracy of the proposed algorithms in tracking the GMPP in each pattern, the mean convergence curves for the tracked PV power, and duty cycle over the number of runs are plotted and reported in Table 3 for the three patterns.

For pattern 1, as illustrated in Fig. 2(a), a single global peak is generated in the P-V characteristics at 148.693 W, and can be observed from Fig. 2(b). This pattern is considered as the most straightforward condition for all the algorithms, since, all PV modules receive an equal amount of irradiation. The mean convergence curves of the power and duty cycle are presented in the first column of Table 3. From these figures, it can be noticed that C-FPA variants converged for a higher value of power with zero oscillations and nearly at 50 % of the time required in the case of FPA. The C-FPA variants logistic, sine and tent maps can track 148.512 W at 1.523 sec, 2.168 sec, and 1.249 sec respectively. However, FPA tracks 144.908 W in 3.333 sec. Also, C-FPA variants show more stable performance as they show zero oscillation around MPP. However, in the case of FPA, continuous oscillations can be observed around MPP until 3.33 sec before starting to converge.

For pattern 2, C-FPA and FPA try to distinguish between the GMPP and LMPP from the PV characteristics as PV string receives two unequal levels of irradiation, as shown in Fig. 2(a). Due to this unequal irradiation, PV system generates two peaks with power values of 69.742 W (GMPP) and 43.978 W (LMPP). The two peaks are highlighted with points P2 and P3, respectively, and are presented in Fig. 2(b). Similar to pattern 1; the obtained mean tracking power and duty cycle plots for pattern 2 are presented in the second column of Table 3. From the figures, it can be seen that FPA converges to power value equaled to 69.623 W in a duration of 2.333 sec and can observe the oscillations around MPP. C-FPA variant with logistic map tracks maximum power of 69.709 W at 0.995 sec. C-FPA with sine and tent maps tracks 69.71 W at 1.316 sec and 1.354 sec, respectively. From the above tracking power and convergence time, it is noteworthy to mention that, a logistic map shows its superiority by taking less time to converge and tracks the high value of power compared to other variants including with FPA.

Finally, pattern 3 is assumed to have a strong shade pattern by considering non-homogeneous irradiation levels on PV string. Sequentially four, peaks are produced in the P-V characteristics and that are indicated with points P4, P5, P6, and P7 as shown in Fig. 2(b). Among the four peaks, point P6 is considered as GMPP with power values of 57.616 W, and other points P4, P5, and P7 are treated as LMPP which generates power of 51.005 W, 46.415 W, and 30.301 W, respectively. Based on the simulation carried out, the obtained mean power and convergence curves for pattern 3 are plotted in the third column of Table 3. From the presented results, it can be seen that FPA tracks mean power of 56.121 W at 3.33 sec with the presence of high oscillation, while the C-FPA with sine map produces power of 57.376 W at 1.228 sec before settling. For C-FPA with logistic and tent maps generates power of 57.4 W in 1.231 sec and 0.769 sec respectively without any oscillations around MPP. Therefore, merging the chaos maps with the basic version of FPA helps in generating high power with reduced tracking time nearly by 70% from consumed time by standard FPA during non-homogeneous irradiation conditions. From the results above, the chaotic tent variant proves its robustness by producing high values of power in shorter tracking time without any oscillations.

2) STATISTICAL COMPARATIVE STUDY

For the extensive verification of the robustness and consistency of the proposed method, the efficiency in tracking the MPP at each second over the entire simulation is determined. To assess the consistency of the proposed methods, the efficiency curves for 10 independent runs for each second by second is plotted and presented in Table 4 for the three patterns. Additionally, a statistical analysis is performed between the three chaotic variants and FPA. For a critical understanding

TABLE 3. Simulated mean power, and duty cycle of FPA and C-FPA variants for 4S PV string for the tested three patterns over the independent number of runs.

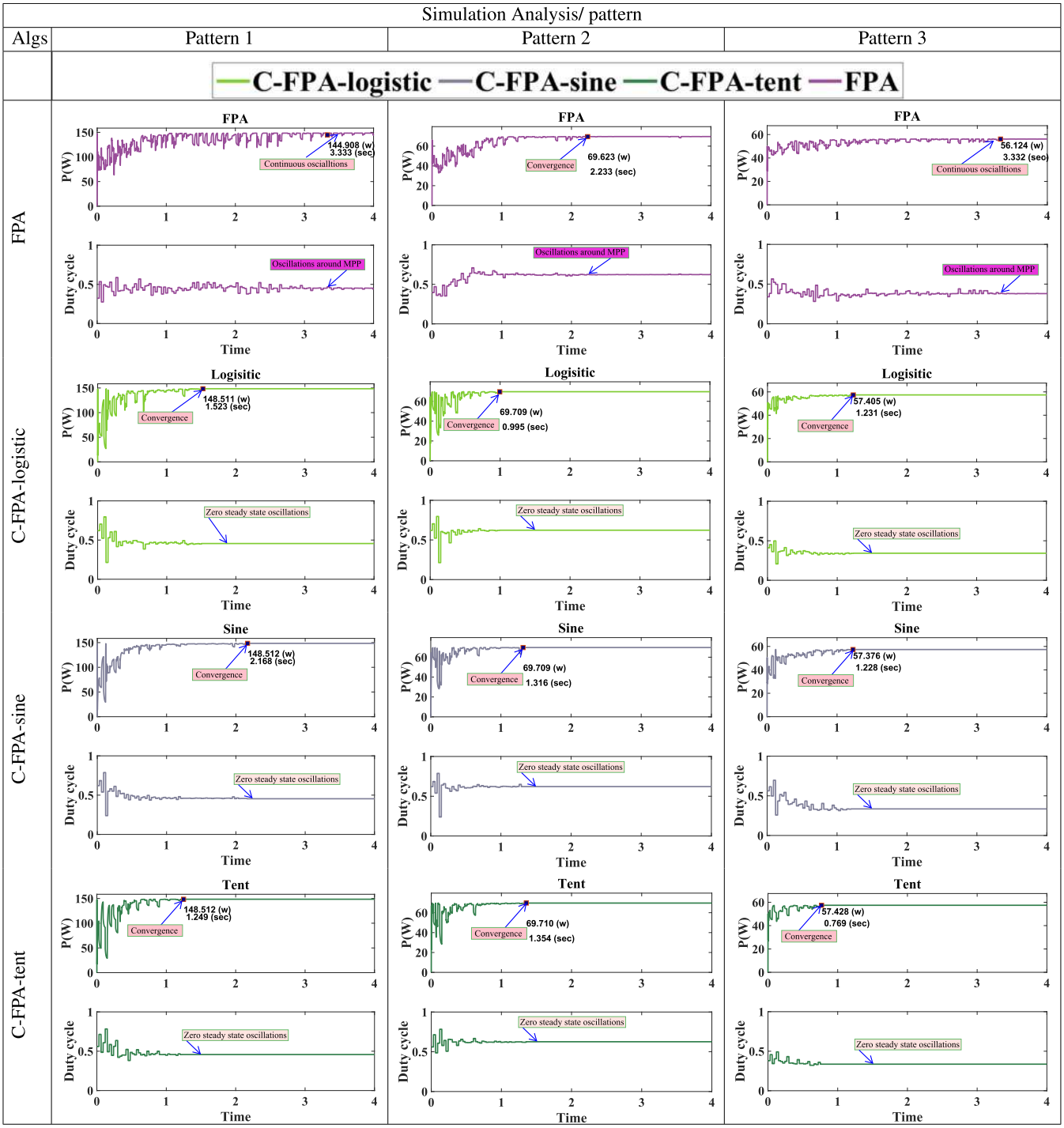

of statistical analysis, the metrics have been calculated and presented in Table. 5.

For Pattern 1, the obtained efficiency curves are presented in 1^{st} row of Table 4. From the efficiency curves, it is observed that the efficiency of FPA is varied from 70 % to 99 % at 1^{st} second and during 2^{nd} and 4^{th} seconds, it varies from 90% to 99%. Whereas, in the case of C-FPA variants, it shows nearly constant efficiency over the entire simulation time. Here, the chaotic tent map achieves the mean efficiency of 99.8789 %. From the above-presented efficiency curves, it reveals that FPA exhibits inconsistency in tracking the GMPP and also achieves less efficiency.

The efficiency curves of pattern 2 are presented in 2^{nd} row of Table 4. Based on the efficiency curves, it is concluded

TABLE 4. Efficiency (η%) over the time of the simulations by the FC-FPA variants and the basic FPA over the number of runs for patterns 1, 2, and 3 of the 4S connected S36 configuration.

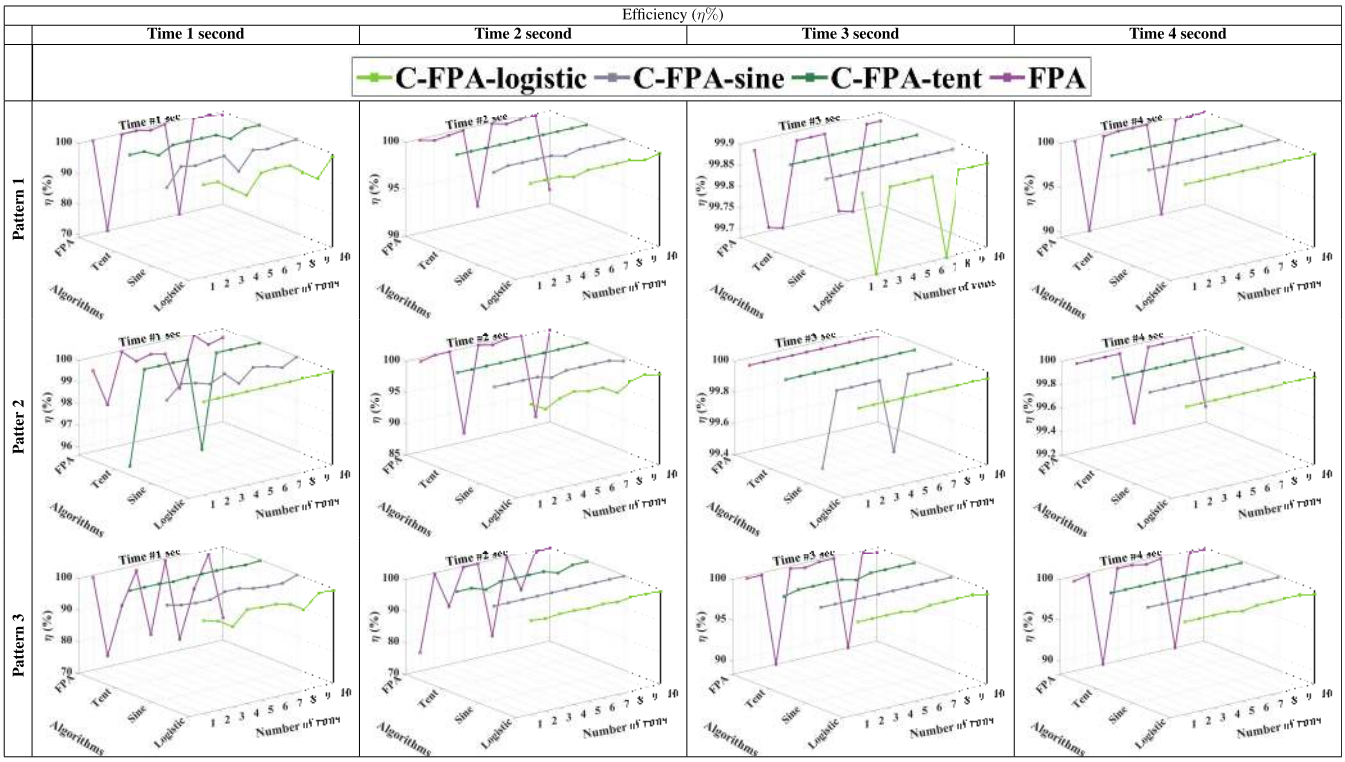

TABLE 5. Comparison between MPPT variants over the three patterns.

PSC patterns/ Algorithms			Comparable factors						
			$Mean(P_{pv_{ei}})(W)$	$P_{pv_m}(W)$	$Mean(\eta)$ (%)	$RMSE$	MAE	STD	Tracking time (sec)
Pattern 1	FPA	**FPA**	144.908		97.4545	7.05646	3.35738	$6.207e+00$	3.333
	C-FPA	**Logistic**	148.512	148.693	99.8783	0.18134	0.18134	$0.000e+00$	1.523
		Sine	148.512		99.8783	0.18134	0.18134	$5.569e-10$	2.168
		Tent	148.512		99.8783	0.18134	0.18134	$5.569e-10$	1.249
Pattern 2	FPA	**FPA**	69.623		99.8294	0.11853	0.20921	$1.724e-01$	2.233
	C-FPA	**Logistic**	69.709	69.742	99.9527	0.03234	0.03234	$2.216e-08$	0.995
		Sine	69.710		99.9541	0.03234	0.03234	$1.224e-08$	1.316
		Tent	69.710		99.9541	0.03234	0.03234	$5.920e-08$	1.354
Pattern 3	FPA	**FPA**	56.121		97.40205	3.00158	1.49683	$2.602e+00$	3.333
	C-FPA	**Logistic**	57.277	57.616	99.4116	0.20295	0.18843	$7.539e-02$	1.231
		Sine	57.465		99.7379	0.15073	0.15073	$3.295e-00$	1.228
		Tent	57.465		99.7379	0.15073	0.15073	$1.351e-07$	0.769

that the C-FPA variants are more efficient and reliable than FPA. The C-FPA provides higher and more consistent values of efficiency overall seconds and for all 10 independent runs. This can be observed, especially in the cases of the tent and logistic maps.

Pattern 3 is tested under hard partial shading conditions. Similar to the above two cases, the plots related to Pattern 3 are presented in 3^{rd} row of Table 4. The FPA efficiency varies between 75% to 99%, while the C-FPA variants perform the high efficiency with fewer variations over entire simulation

TABLE 6. The best and worst run for each algorithm over each step change in irradiance condition from pattern 1 to pattern 3.

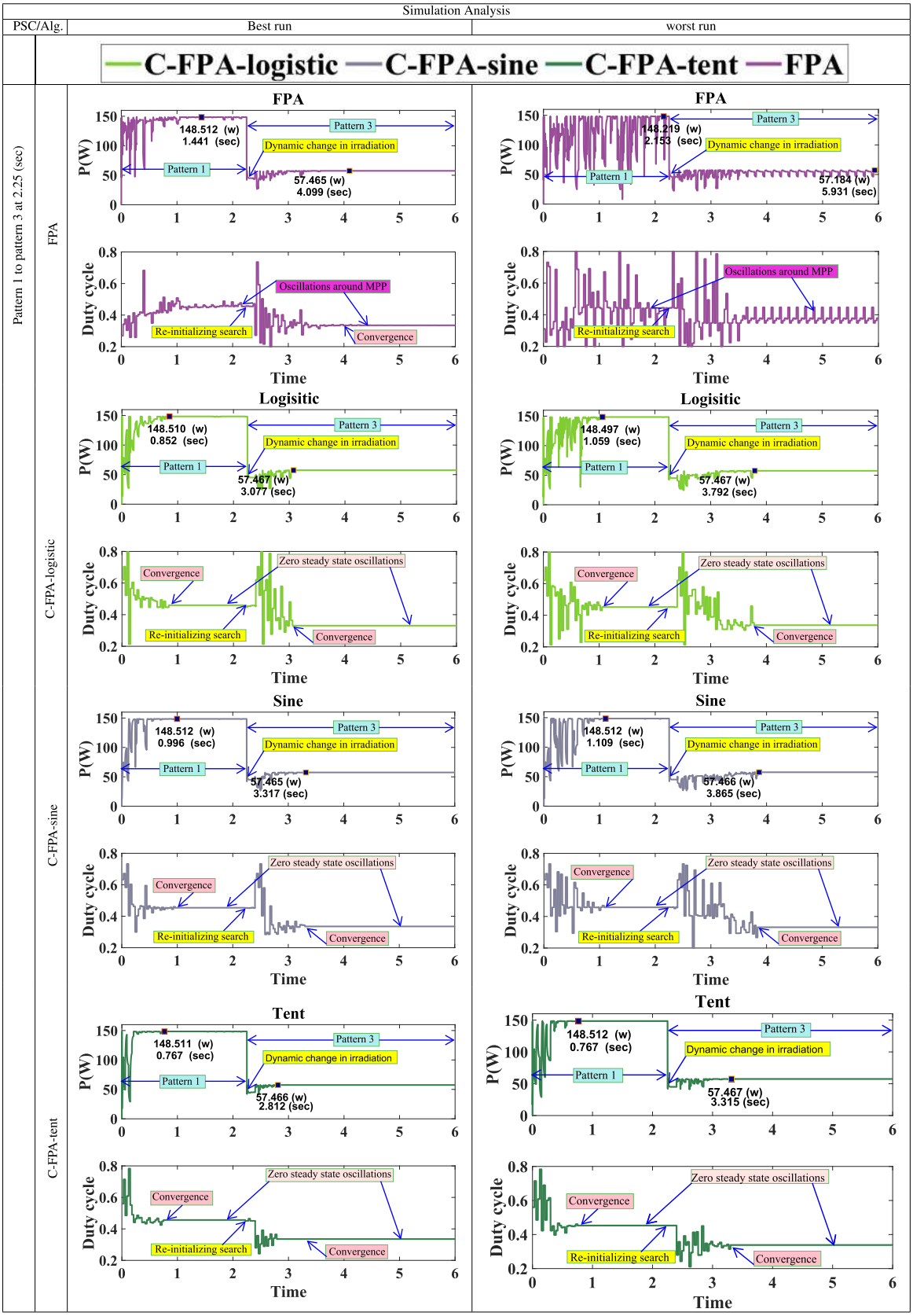

TABLE 7. The best and worst run for each algorithm over each step change in irradiance condition from pattern 2 to pattern 3.

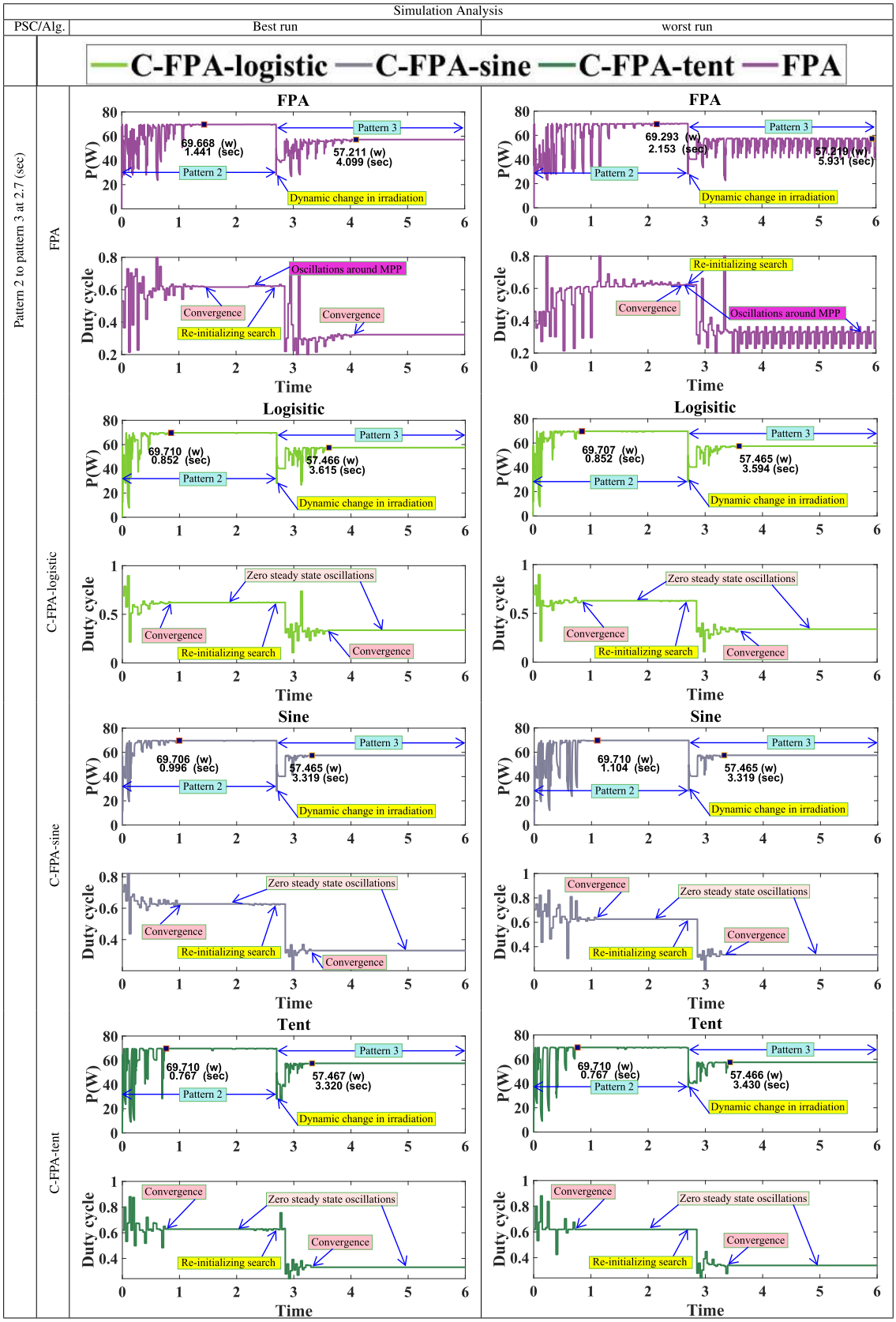

time for 10 independent runs. Thereby it can be concluded that C-FPA variants show robust, superior performance, high efficiency, consistency in tracking GMPP over FPA irrespective of shade conditions.

In addition to the efficiency curves, the performance indicators were also calculated using formulae presented in (12), (13), (14). The obtained values for 3 patterns are presented in Table 5. From the results presented in Table 5, it is understood that the RMSE value of FPA for pattern1 is 7.05646, which is much higher than C-FPA RMSE values, which in the range of 0.18134. Similarly, the achieved efficiency by C-FPA variants are also higher than FPA; it indicates the superior performance of C-FPA variants. For pattern 3, the mean efficiency of the C-FPA tent map achieves 99.737 % with a tracking time of 0.769 seconds in spite of the rigorous partial shading conditions. The values of STD ($STD = 1.351 \times 10^{-7}$) shows high consistency of the method than other variants including with FPA. Consequently, the chaos maps enhance the exploration phase of the standard algorithm that helps in avoiding to settle in the LMPP in a short time.

By the end of this subsection, it is evident that cooperating the chaos maps into the FPA for the initialization, and the adaptive adjusting of its parameters increase the consistency of the algorithm under all shade conditions. Moreover, C-FPA variants provide higher power than FPA with least tracking time, that equal to 50 % of FPA especially tent map for the 1^{st} and 3^{rd} pattern and all of the maps for pattern 2.

B. SIMULATION STUDY UNDER THE DYNAMIC CHANGE IN IRRADIATION

In continuation to the previous test conditions, the developed algorithms were also tested under a dynamic change in irradiation conditions to strengthen the superiority, robustness, reliability, and efficiency of proposed variants (C-FPA). In practical and real-time conditions, the PV array experiences dynamic variations in shade due to the change in environmental conditions. So, testing under dynamic change conditions become essential. Therefore, in this work, step change in the irradiation is considered at different samples of time under two cases.

In the 1^{st} case, the incident irradiation levels on the PV string is changed from the uniform distribution as in pattern 1 to partial shading condition as in pattern 3. Each algorithm is simulated for 10 independent runs over the previously mentioned stages. The best and worst tracking performance by each technique is plotted in Tables. 6. In this case, the irradiation levels changed from pattern 1 to pattern 3 at 2.25 sec and it is highlighted in figures with dynamic change in irradiation. Due to change in irradiation, the algorithm start to reinitialize itself to track the MPP in shorter time. The position of reinitializing search can observed from the plotted curves. From the plotted best and worst run figures in Table 6, it can be notice that, chaotic variant tent map get converge in 0.767 sec and generates maximum power in both best and worst run conditions. But, in case of FPA for best run, it takes 1.441 sec to get converge. However in worst run condition, it is not able to get converge even after 2.153 sec and there exist huge oscillations around MPP. The occurrence of oscillations are fully nullified in C-FPA variants.

In 2^{nd} case, the PV string is experienced for variations between two partial shading conditions from pattern 2 to pattern 3. The irradiation levels on the PV array changes from pattern 2 to pattern 3 suddenly after 2.7 sec. Simulation has been carried-out for 10 ten independent runs, and the obtained best, worst power and duty cycle curves were presented in Table 7. The best and worst convergence curves in Table 7 show that a noticed deviation between the best and worst runs of the FPA, whereas in C-FPA variants this drawback is sorted-out and provides more consistent and close results over all the number of the independent runs. Moreover, C-FPA variants are so sensitive for the variations in irradiation levels as they consume a shorter time to track the GMPP than FPA with least oscillation. FPA fluctuates around MPP trying to get convergence while that takes many seconds which reflects on the efficiency of the MPP tracker system.

It is clear from the results that, the best-tracked power values by FPA are less than the worst one by the C-FPA variants. Further FPA executes longer tracking time. On the other hand, the best and worst runs of C-FPA are much close in the extracted power, efficiency and tracking time especially in case of tent map as reported in Tables.6, and 7. Accordingly, it can be concluded that combining the tent map with FPA has several merits as it reduces the tracking time about 50 % from that required by FPA, it increases the stability and the efficiency of the GMPP tracking system, as well as it provides a better dynamic response for the MPPT novel method (C-FPA).

V. CONCLUSION

Novel GMPP tracking technique variants are proposed in the current manuscript to tackle several drawbacks of the traditional algorithms. The noticeable hiccups are instability and the high oscillation in the tracking process, tripping in the LMPP in partial shade conditions and the tracking time. In the new approach, three chaos maps (Logistic, sine, and tent maps) are merged with the Flower Pollination Algorithm to tune some of its parameters and generating the initial solution. As a result, Chaotic Flower Pollination Algorithm (C-FPA) variants are introduced and tested in tracking GMPP over several shade conditions moreover over the step variations in the irradiance conditions. The developed variants response is compared with FPA based on several statistical analysis to show the influence of integrating the chaos maps in the tracking system. The overall outcome shows that C-FPA variants can track the GMPP efficiently and with higher extracted power and shorter tracking time than FPA as well as C-FPA offers a more stable and fast dynamic response.

ACKNOWLEDGMENT

The authors would like to thank the reviewers and associate editor for their valuable comments and recommendations to improve the quality of the article.

REFERENCES

[1] T. S. Babu, N. Rajasekar, and K. Sangeetha, "Modified particle swarm optimization technique based maximum power point tracking for uniform and under partial shading condition," *Appl. Soft Comput.*, vol. 34, pp. 613–624, Sep. 2015.

[2] S. Hadji, J.-P. Gaubert, and F. Krim, "Real-time genetic algorithms-based MPPT: Study and comparison (theoretical an experimental) with conventional methods," *Energies*, vol. 11, no. 2, p. 459, 2018.

[3] T. S. Babu, J. P. Ram, T. Dragi ević, M. Miyatake, F. Blaabjerg, and N. Rajasekar, "Particle swarm optimization based solar PV array reconfiguration of the maximum power extraction under partial shading conditions," *IEEE Trans. Sustain. Energy*, vol. 9, no. 1, pp. 74–85, Jan. 2018.

[4] S. N. Deshkar, S. B. Dhale, J. S. Mukherjee, T. S. Babu, and N. Rajasekar, "Solar PV array reconfiguration under partial shading conditions for maximum power extraction using genetic algorithm," *Renew. Sustain. Energy Rev.*, vol. 43, pp. 102–110, Mar. 2015.

[5] M. Gokdag, M. Akbaba, and O. Gulbudak, "Switched-capacitor converter for PV modules under partial shading and mismatch conditions," *Sol. Energy*, vol. 170, pp. 723–731, Aug. 2018.

[6] F. Wang, T. Zhu, F. Zhuo, H. Yi, S. Shi, and X. Zhang, "Analysis and optimization of flexible MCPT strategy in submodule PV application," *IEEE Trans. Sustain. Energy*, vol. 8, no. 1, pp. 249–257, Jan. 2017.

[7] S. Strache, R. Wunderlich, and S. Heinen, "A comprehensive, quantitative comparison of inverter architectures for various PV systems, PV cells, and irradiance profiles," *IEEE Trans. Sustain. Energy*, vol. 5, no. 3, pp. 813–822, Jul. 2014.

[8] A. N. A. Ali, M. H. Saied, M. Z. Mostafa, and T. M. Abdel-Moneim, "A survey of maximum PPT techniques of PV systems," in *Proc. IEEE Energytech*, May 2012, pp. 1–17.

[9] C. Huang, L. Wang, H. Long, X. Luo, and J.-H. Wang, "A hybrid global maximum power point tracking method for photovoltaic arrays under partial shading conditions," *Optik*, vol. 180, pp. 665–674, Feb. 2019.

[10] J. P. Ram, T. S. Babu, and N. Rajasekar, "A comprehensive review on solar PV maximum power point tracking techniques," *Renew. Sustain. Energy Rev.*, vol. 67, pp. 826–847, Jan. 2017.

[11] M. Seyedmahmoudian, T. K. Soon, E. Jamei, G. S. Thirunavukkarasu, B. Horan, S. Mekhilef, and A. Stojcevski, "Maximum power point tracking for photovoltaic systems under partial shading conditions using bat algorithm," *Sustainability*, vol. 10, no. 5, p. 1347, 2018.

[12] N. Aouchiche, M. S. Aitcheikh, M. Becherif, and M. A. Ebrahim, "Ai-based global MPPT for partial shaded grid connected PV plant via MFO approach," *Sol. Energy*, vol. 171, pp. 593–603, Sep. 2018.

[13] J. P. Ram and N. Rajasekar, "A novel flower pollination based global maximum power point method for solar maximum power point tracking," *IEEE Trans. Power Electron.*, vol. 32, no. 11, pp. 8486–8499, Nov. 2017.

[14] H. Armghan, I. Ahmad, A. Armghan, S. Khan, and M. Arsalan, "Backstepping based non-linear control for maximum power point tracking in photovoltaic system," *Sol. Energy*, vol. 159, pp. 134–141, Jan. 2018.

[15] R. Gayathri and G. A. Ezhilarasi, "Golden section search based maximum power point tracking strategy for a dual output DC-DC converter," *Ain Shams Eng. J.*, vol. 9, no. 4, pp. 2617–2630, 2018.

[16] K. Sangeetha, T. S. Babu, and N. Rajasekar, "Fireworks algorithm-based maximum power point tracking for uniform irradiation as well as under partial shading condition," in *Artificial Intelligence and Evolutionary Computations in Engineering Systems*. New Delhi, India: Springer, 2016, pp. 79–88.

[17] O. Abdalla, H. Rezk, and E. M. Ahmed, "Wind driven optimization algorithm based global MPPT for PV system under non-uniform solar irradiance," *Sol. Energy*, vol. 180, pp. 429–444, Mar. 2019.

[18] A. Fathy and H. Rezk, "A novel methodology for simulating maximum power point trackers using mine blast optimization and teaching learning based optimization algorithms for partially shaded photovoltaic system," *J. Renew. Sustain. Energy*, vol. 8, no. 2, 2016, Art. no. 023503.

[19] M. A. Mohamed, A. A. Z. Diab, and H. Rezk, "Partial shading mitigation of PV systems via different meta-heuristic techniques," *Renew. Energy*, vol. 130, pp. 1159–1175, Jan. 2019.

[20] K. S. Tey, S. Mekhilef, M. Seyedmahmoudian, B. Horan, A. T. Oo, and A. Stojcevski, "Improved differential evolution-based MPPT algorithm using SEPIC for PV systems under partial shading conditions and load variation," *IEEE Trans. Ind. Informat.*, vol. 14, no. 10, pp. 4322–4333, Oct. 2018.

[21] L. Guo, Z. Meng, Y. Sun, and L. Wang, "A modified cat swarm optimization based maximum power point tracking method for photovoltaic system under partially shaded condition," *Energy*, vol. 144, pp. 501–514, Feb. 2018.

[22] S. Veerapen, H. Wen, X. Li, Y. Du, Y. Yang, Y. Wang, and W. Xiao, "A novel global maximum power point tracking algorithm for photovoltaic system with variable perturbation frequency and zero oscillation," *Sol. Energy*, vol. 181, pp. 345–356, Mar. 2019.

[23] H. Chaieb and A. Sakly, "A novel MPPT method for photovoltaic application under partial shaded conditions," *Sol. Energy*, vol. 159, pp. 291–299, Jan. 2018.

[24] M. Alshareef, Z. Lin, M. Ma, and W. Cao, "Accelerated particle swarm optimization for photovoltaic maximum power point tracking under partial shading conditions," *Energies*, vol. 12, no. 4, p. 623, 2019. [Online]. Available: http://www.mdpi.com/1996-1073/12/4/623

[25] M. Mao, Q. Duan, P. Duan, and B. Hu, "Comprehensive improvement of artificial fish swarm algorithm for global MPPT in PV system under partial shading conditions," *Trans. Inst. Meas. Control*, vol. 40, no. 7, pp. 2178–2199, 2018.

[26] A. M. Eltamaly and H. M. Farh, "Dynamic global maximum power point tracking of the PV systems under variant partial shading using hybrid GWO-FLC," *Sol. Energy*, vol. 177, pp. 306–316, Jan. 2019.

[27] M. Mao, L. Zhang, P. Duan, Q. Duan, and M. Yang, "Grid-connected modular PV-converter system with shuffled frog leaping algorithm based DMPPT controller," *Energy*, vol. 143, pp. 181–190, Jan. 2018.

[28] J. P. Ram, D. S. Pillai, N. Rajasekar, and S. M. Strachan, "Detection and identification of global maximum power point operation in solar PV applications using a hybrid ELPSO-P&O tracking technique," *IEEE J. Emerg. Sel. Topics Power Electron.*, to be published.

[29] M. N. Bhukya and V. R. Kota, "A quick and effective mppt scheme for solar power generation during dynamic weather and partial shaded conditions," *Eng. Sci. Technol., Int. J.*, vol. 22, no. 3, pp. 869–884, 2019.

[30] M. Mao, L. Zhou, Z. Yang, Q. Zhang, C. Zheng, B. Xie, and Y. Wan, "A hybrid intelligent GMPPT algorithm for partial shading PV system," *Control Eng. Pract.*, vol. 83, pp. 108–115, Feb. 2019.

[31] E. Amer, A. Kuperman, and T. Suntio, "Direct fixed-step maximum power point tracking algorithms with adaptive perturbation frequency," *Energies*, vol. 12, no. 3, p. 399, 2019.

[32] D. Pilakkat and S. Kanthalakshmi, "An improved p&o algorithm integrated with artificial bee colony for photovoltaic systems under partial shading conditions," *Sol. Energy*, vol. 178, pp. 37–47, Jan. 2019.

[33] H. Hamdi, C. B. Regaya, and A. Zaafouri, "Real-time study of a photovoltaic system with boost converter using the PSO-RBF neural network algorithms in a MyRio controller," *Sol. Energy*, vol. 183, pp. 1–16, May 2019.

[34] M. Al-Dhaifallah, A. M. Nassef, H. Rezk, and K. S. Nisar, "Optimal parameter design of fractional order control based INC-MPPT for PV system," *Sol. Energy*, vol. 159, pp. 650–664, Jan. 2018.

[35] S. Mirjalili and A. H. Gandomi, "Chaotic gravitational constants for the gravitational search algorithm," *Appl. Soft Comput.*, vol. 53, pp. 407–419, Apr. 2017.

[36] D. Yousri, D. Allam, M. B. Eteiba, and N. Suganthan, "Static and dynamic photovoltaic models' parameters identification using Chaotic Heterogeneous Comprehensive Learning Particle Swarm Optimizer variants," *Energy Convers. Manage.*, vol. 182, pp. 546–563, Feb. 2019. [Online]. Available: http://www.sciencedirect.com/science/article/pii/S0196890418313566

[37] D. Yousri, A. M. AbdelAty, L. A. Said, A. S. Elwakil, B. Maundy, and A. G. Radwan, "Chaotic flower pollination and grey wolf algorithms for parameter extraction of bio-impedance models," *Appl. Soft Comput.*, vol. 75, pp. 750–774, Feb. 2019.

[38] D. Yousri, D. Allam, and M. B. Eteiba, "Chaotic whale optimizer variants for parameters estimation of the chaotic behavior in permanent magnet synchronous motor," *Appl. Soft Comput.*, vol. 74, pp. 479–503, Jan. 2019.

[39] M. Gao, J. Shen, and J. Jiang, "Visual tracking using improved flower pollination algorithm," *Optik*, vol. 156, pp. 522–529, Mar. 2018.

[40] D. F. Alam, D. A. Yousri, and M. B. Eteiba, "Flower pollination algorithm based solar PV parameter estimation," *Energy Convers. Manage.*, vol. 101, no. 1, pp. 410–422, Sep. 2015.

[41] M. M. Samy, S. Barakat, and H. S. Ramadan, "A flower pollination optimization algorithm for an off-grid PV-fuel cell hybrid renewable system," *Int. J. Hydrogen Energy*, vol. 44, no. 4, pp. 2141–2152, 2018.

[42] X.-S. Yang, "Flower pollination algorithm for global optimization," in *Proc. Int. Conf. Unconv. Comput. Natural Comput.* Berlin, Germany: Springer, 2012, pp. 240–249.

[43] J. Yi, D. Jian, and S. Zhenhong, "Pattern synthesis of MIMO radar based on chaotic differential evolution algorithm," *Optik*, vol. 140, pp. 794–801, Jul. 2017.

[44] S. Yaghoobi and H. Mojallali, "Tuning of a PID controller using improved chaotic krill herd algorithm," *Optik*, vol. 127, no. 11, pp. 4803–4807, 2016.
[45] L. Hongtao and K. Fengju, "Adaptive chaos parallel clonal selection algorithm for objective optimization in WTA application," *Optik*, vol. 127, no. 6, pp. 3459–3465, 2016.
[46] R. M. May, "Simple mathematical models with very complicated dynamics," *Nature*, vol. 261, no. 5560, pp. 459–467, 1976.
[47] B. V. Chirikov, "A universal instability of many-dimensional oscillator systems," *Phys. Rep.*, vol. 52, no. 5, pp. 263–379, May 1979.

DALIA YOUSRI received the B.Sc. degree (Hons.) from the Electric Power and Machine Department, Faculty of Engineering, Fayoum University, Egypt, in 2011, and the M.Sc. degree, in 2016. From 2013 to 2016, she was a Demonstrator with the Electric Power and Machine Department, Faculty of Engineering, Fayoum University, where she has been currently a Teaching Assistant, since June 2016. She has published refereed journals on PV modeling and modifying the optimization algorithms with different applications. Her fields of interests include photovoltaic modeling, photovoltaic system design, and optimization algorithms.

THANIKANTI SUDHAKAR BABU received the B.Tech. degree from Jawaharlal Nehru Technological University, Ananthapur, India, in 2009, the M.Tech. degree in power electronics and industrial drives from Anna University, Chennai, India, in 2011, and the Ph.D. degree from VIT University, Vellore, India, in 2017. He is currently a Postdoctoral Researcher with the Department of Electrical Power Engineering, Institute of Power Engineering, Universiti Tenaga Nasional (UNITEN), Malaysia. He has published more than 30 research articles in various reputed international journals. Acting as editorial board members and reviewers for various reputed journals, such as the IEEE and the IEEE Access, IET, Elsevier and Taylor and Francis. His areas of interests include design and implementation of solar PV systems, renewable energy resources, power management for hybrid energy systems, fuel cell technologies, electric vehicle, and smart grid.

DALIA ALLAM received the B.Sc., M.Sc., and Ph.D. degrees in electrical power engineering from Cairo University, Egypt. She was certified as a Siemens Trainer in several automation subjects. She was an Ex-manager of the Automatic Control Unit, Fayoum University, Egypt, where she is currently an Associate Professor with the Electrical Engineering Department. Her areas of interests include applications of AI and SI in electrical power engineering, renewable energy, power quality, smart relays and digital protection systems, and automation and process control. She is also a Reviewer for many international journals.

VIGNA K. RAMACHANDARAMURTHY (SM'12) received the Ph.D. degree in electrical engineering from the Institute of Science and Technology, The University of Manchester, U.K., in 2001.

He is currently a Professor with the Institute of Power Engineering, Universiti Tenaga Nasional, Malaysia. He is also a Chartered Engineer registered with the Engineering Council of U.K., and a Professional Engineer registered with the Board of Engineers, Malaysia. He is also the Principal Consultant for Malaysia's biggest electrical utility, Tenaga Nasional Berhad, and has completed over 250 projects in renewable energy. He has also developed several technical guidelines for distributed generation, Malaysia. He is also in the editorial board/associate editor of *IET Smart Grid*, IET RPG, the IEEE Smart Grid, and IEEE Access. His areas of interests include power systems related studies, renewable energy, energy storage; power quality, electric vehicle, and rural electrification.

MAGDY B ETIBA was born in Cairo, Egypt. He received the B.Sc. and M.Sc. degrees in electrical power from Ain Shams University, Cairo, Egypt, in 1970 and 1975, respectively, and the M.Eng. and Ph.D. degrees in electrical power from McGill University, Montreal, QC, Canada, in 1977 and 1982, respectively.

He is currently a Professor with the Department of Electrical Engineering and an Ex vice dean for student affairs, Fayoum University, Fayoum, Egypt. He has published many papers and articles in international journals and conferences. His research interests include insulation and thermal characteristics of high-voltage equipment, transmission lines and cables, and applications of renewable energy resources in the power sector. Dr. Eteiba was a member of the National Committee for Higher Education Enhancement, Egypt.